Article

Not peer-reviewed version

Analytical Model of Thread Turning Insert for Workpieces with Different Machinability

Cristian Barz , Oleh Onysko * , Volodymyr Kopei , Yaroslav Kusyi , Lesia Shkitsa , Predrag Dašić , Saulius Baskutis

Posted Date: 3 March 2026

doi: 10.20944/preprints202603.0123.v1

Keywords: trapezoidal thread; flank angle; rake angle; inclination angle; lead screw; buttress thread; deviation

 doi:10.20944/preprints202603.0123.v1

Article

Analytical Model of Thread Turning Insert for Workpieces with Different Machinability

Cristian Barz [1], Oleh Onysko [2,*], Volodymyr Kopei [3], Yaroslav Kusyi [3], Lesia Shkitsa [4], Predrag Dašić [5] and Saulius Baskutis [6]

[1] North University Centre of Baia Mare, Technical University of Cluj-Napoca, Victor Babes str., no.62A.,430083 Baia Mare, Romania

[2] Department of Computerized Mechanical Engineering, Ivano-Frankivsk National Technical University of Oil and Gas, Karpatska str., no. 15, 76019 Ivano-Frankivsk, Ukraine

[3] Department of Computerized Mechanical Engineering, Ivano-Frankivsk National Technical University of Oil and Gas, Karpatska str., no. 15, 76019 Ivano-Frankivsk, Ukraine

[4] Institute of Engineering Mechanics and Robotics, Ivano-Frankivsk National Technical University of Oil and Gas, Karpatska str., no. 15, 76019 Ivano-Frankivsk, Ukraine

[5] Engineering Academy of Serbia (IAS), Str. Kneza Miloša 9/IV, 11000 Belgrade, Serbia

[6] Kaunas University of Technology, Department of Production Engineering, 56, Studentu St., Kaunas 51424, Lithuania

* Correspondence: oleh.onysko@nung.edu.ua

Abstract

Modern requirements for critical threads, such as drilling lock threads or running trapezoidal threads of heavy machine tools dictate the need for very durable and at the same time very accurate thread cutters. Conventional thread cutters supplied to the world market have the same profile as the thread for which they are intended. However, for durability and productivity, such tools should have effective geometric parameters of the cutting part, namely: the rake angle and the angle of inclination of the cutting edge. However, there are no known algorithms for profiling such cutters in order to ensure their maximum possible accuracy. This analytical study is specifically designed to identify an algorithm that makes it possible to make highly productive and at the same time highly accurate thread cutters with straight sides of the profile for the manufacture of threads with trapezoidal, triangular and buttress profiles, including for parts made of difficult-to-machine materials.

Keywords: trapezoidal thread; flank angle; rake angle; inclination angle; lead screw; buttress thread; deviation

1. Introduction

The modern process of research of hydrocarbon [1], geothermal [2], water [3] and soil resources [4], as well as environmental [5], recreational monitoring [6] and scientific research of subsoil and development of underground infrastructure of large cities [7] is in the focus of public attention. The key technological tool in these processes is drill strings [8], long elastic systems with a large number of threaded connections [9], which ensure mechanical integrity and tightness of the columns in difficult well conditions [10]. Therefore, increased requirements are imposed on the strength of the connection material [11] and at the same time on its accuracy [12]. At the same time, the main advantage of threaded connections, namely the possibility of multiple assembly and disassembly, sometimes turns into a source of failures: self-unscrewing under the influence of vibration-cyclic loads [13], violation of the tightness of sealing areas [14], accelerated wear, etc. [15]. As a result, downtime, maintenance costs and the risk of accidents increase. One of the key factors limiting the effectiveness of deep and directional drilling is uncontrolled dynamics of the drill string [16]: torsional vibrations [17], as well as axial and transverse vibrations [18]. Dynamic loads accelerate the

 doi:10.20944/preprints202603.0123.v1

wear of bits [19] and downhole equipment [20], worsen the operation of threaded connections [21], and affect the resource of engines and ground systems [22]. A well-known approach to solving this problem is based on the use of special vibration-proof devices [23]: drilling shock absorbers and dampers [24], elastic spindles [25], downhole motors, etc. [26]. This improves the operating modes of threaded connections, but does not eliminate the root causes of the problems. The operating environment of drill strings is characterized by abrasiveness, corrosive aggressiveness, high pressures and temperatures, as well as the action of long-term cyclic loads [27,28]. The increase in the depth and complexity of well trajectories places special demands on materials, smart structures and modern technologies for designing and manufacturing connections [29] - from the level of microgeometry to controlled residual stresses and roughness parameters [30], which determine tightness [31] and sensitivity to fatigue failure [32]. From the point of view of continuum mechanics [33], threaded profiles contain sharp-ended stress concentrators [34,35]. The stress-strain state of pipes and cylindrical shells near such concentrators in contact has been studied in detail in [35,36], which is directly relevant for the analysis of the thread root [35] and first thread turns [36,37].

All of the above operational requirements and conditions pose the corresponding tasks of modernization of machining for manufacturers of heavily loaded threads. Therefore, a significant analysis of the machining process of parts that are: mass-produced and are functionally responsible is needed. For example, the improvement of machine tools proves that it is possible to significantly increase productivity without actually losing accuracy [38], and the applied modular approach enhances optimization in the design of machine tools [39]. In addition, a significant contribution to the intensification of parts manufacturing is a scientifically based technological route, which allows significantly optimizing the process of creating threaded parts [40,41], as well as effective management of the life cycle of production assets [42]. However, the first priority is the modernization of cutting tools themselves: from the methods of their application to their geometric parameters [43].

2. Review of the Thread Turning Achievements and Problems. Aim of Research

Studies on thread cutting in AISI 304L stainless steel indicate that an important argument for reducing cutter wear is the use of a combined infeed method (incremental feed) [44]. In [45], a significant increase in cutter stability in the process of turning a critical buttress thread from high-chromium stainless steel was proven by using a positive rake angle of 12°. To increase the accuracy of threads, it is important to control profile deviations caused by deformations [46]. In studies [47,48], modeling the tool trajectory during thread turning, taking into account the influence of vibration, made it possible to increase the stability of the cutting edge profile. The aim of the study [49] is to increase the productivity of turning high-quality threaded aluminum parts. To achieve this goal, the front surface of the cutter was supplemented with micro-holes using a laser to retain solid lubricating micro and nano materials in them. Vector analysis predicting tangential and radial deviations of conical screw surfaces [50] shows possible ways to improve thread turning processes. A large number of input technological parameters were taken into account in a scientific study of the surface condition of the external thread on an aviation part made of the difficult-to-machine material Incolonel 718 [51]. In [52], tests of turning titanium alloy threads showed the effective effect of a cryogenic environment on reducing the amount of tool blade wear. The study [52] also concerned the development of a mathematical model of cutter wear to determine the expected tool life. Measurement of the profile of the resulting thread and determination of its accuracy using a special device was proposed in [53]. In contrast to measurement, in the analytical work [54], an algorithm for calculating the conical thread profile depending on the geometric parameters of the blade of a turning thread cutter with deviations is presented. The geometric three-dimensional thread turning simulator developed on the basis of FreeCAD [55] can serve as a check or supplement to the analytical algorithm proposed in the work [54]. These results show the formation of a convex or concave thread profile instead of the expected rectilinear one. Based on the kinematics of the process of forming a conical helical surface, a method is proposed that enables the accurate formation of the screw pitch as a function of the angle of rotation

 doi:10.20944/preprints202603.0123.v1

of the part [56]. The study [57] presents an analysis of the movements of the cutting blade of the cutter during the process of turning a conical thread. The formation of helical linear surfaces and the accuracy of worm manufacturing are closely related to the influence of geometric parameters, including the angle of inclination of the helix. Therefore, approximate forms of mathematical models of helicoid accuracy are often used [58]. Measuring the accuracy of the lead screw thread pitch by the traditional method and by the method that takes into account the axial displacement of the shaft indicates a higher accuracy of the latter [59]. This is important for precision threads. The measuring and testing base of mechanical processing increasingly uses advanced thermoelectric and photovoltaic materials [60,61]. In [62], it is proposed to design a variety of cutting tools, including threaded ones, automatically using the developed surface generation method. Thread turning is a special type of cutting that requires in-depth research using systems for measuring and analyzing cutting forces [63]. Turning is always accompanied by high temperatures at the tip of the cutter blade. In [64], the cutting of low-alloy hardened steel in dry and minimum-lubrication conditions (MQL) was investigated. As the source [65] proves, the size of both the wear crater and the side wear of the cutting part directly depend on the duration of the cutting process with the insert. Therefore, the quality of the cutting insert for thread turning depends on the operating conditions: technological parameters (speed, feed, depth), cutting methods (profile, generator, combined), methods and types of lubrication and cooling, additional influencing factors (forced vibrations, cryogenic environments), as well as on the design of the tool, which takes into account all the listed factors.

Global manufacturers of cutting tools offer carbide inserts for thread turning only with a zero rake angle (Figure 1a) [66]. However, one of the most influential factors that increase the efficiency of thread turning is the use of a non-zero rake angle of the cutter. Scientific and technical studies prove its effectiveness, especially in the manufacture of parts from difficult-to-machine materials [44,45] (Figures 1b, 1c).

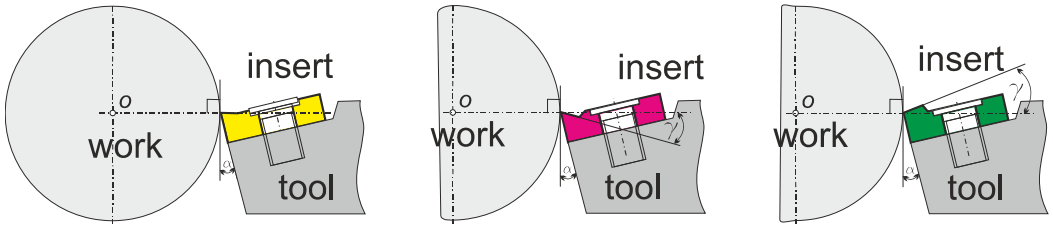

(a) (b) (c)

Figure 1. Scheme of forming geometric parameters when turning a part with a turning tool (α – clearance angle, γ – rake angle): a) γ=0; b) γ>0; c) γ<0;.

According to primary sources [67,68], the value of the rake angle, together with the cutting speed, has a significant impact on the stability of the cutter during turning (Figure 2).

Despite the fact that standard thread cutters have only zero values of rake angles, recommendations on the values of rake angles for thread turning in workpieces made of various materials are widespread in the metalworking information space (Table 1).

Table 1. Rake Angle Versus Material.

No	Workpiece material	Rake angle, deg
1	Steel	12-20
2	Stainless Steel	8-10
3	Aluminum	20-25
4	Titanium	0-4

 doi:10.20944/preprints202603.0123.v1

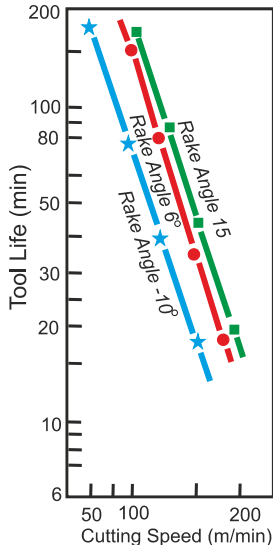

Figure 2. Diagram of the dependence of tool life on cutting speed and rake angle: cutting depth 1 mm, feed 0.32 mm/rev, material: alloy steel, Grade: ST10.

However, it is obvious that the practice of using cutters with a non-zero rake angle is associated with significant possible deviations of the resulting threads in terms of average diameter, pitch, and especially profile [54,55]. In addition, in the case of large-pitch threads (i.e., when the helix has a large lead angle), there is a need to use a non-zero inclination angle of the cutting edge, which increases the deviation of the thread profile [58].

Therefore, the purpose of the study is to analytically determine the profile of a carbide insert for high-precision thread turning with minimal profile deviations depending on the geometric parameters of the thread and the tool (rake angle and cutting edge inclination angle).

3. Profile Accuracy of the Large Pitch Thread for Heavy Using Conditions

Threads with large helix angles, which are most often used in heavily loaded and critical screw pairs, can be divided into three groups according to their profile: conical threads for drill strings of a triangular profile, lead threads for kinematic pairs of a trapezoidal profile (for example, lead screws for metal-cutting machines), dynamic lead screws with a wedge-shaped buttress thread (for example, for hydraulic presses and jacks).

3.1. Profile of Conical Lock Thread According to the API and GOST Standards

Rotary drill string is a threaded drill pipe designed to transmit high torque from the ground rotor to the drill bit at the bottom of the string. In addition, a high-pressure flushing solution (up to 20 MPa) is supplied inside the string from top to bottom. An additional operational requirement is the need for multiple screwing and unscrewing of the pipes during the string lowering and lifting operations to replace a worn bit or for repair. All this together imposes high requirements on the accuracy of the tool-joint conical thread, especially its profile. The strength of the connection, its tightness and unhindered multiple screwing depend on this.

According to ANSI/API standards [69] and GOST standard [70] (Figure 3), such threads are made with nominal pitches P: 4.233 mm, 5.080 mm, 6.35 mm. Diameters d_{2t} (pitch diameter) have values from 30 to 203 mm at the larger base of the cone. The thread flank angle (half profile angle) $\varphi/2 = 30° \pm 45'$ (Figure 3).

 doi:10.20944/preprints202603.0123.v1

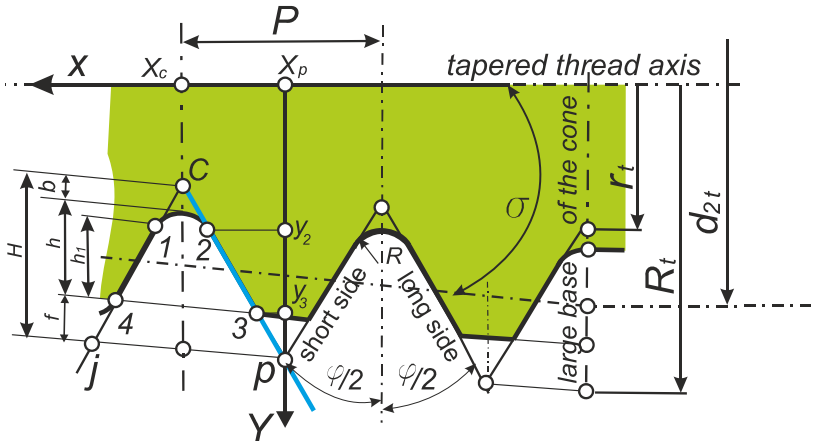

Figure 3. Scheme of a triangular conical thread according to the ANSI/API SPECIFICATION 7-2 standard [69] and GOST [70]. Parameters: φ/2 – flank angle, H – height of fundamental triangle, P – pitch, h – height of the thread, h_1 – height of the profile; f – truncation at crest, b – truncation at root; R – root radius. Dimensions of the larger base of the cone: r_t – minor radius of fundamental triangle, R_t – major radius of fundamental triangle, d_{2t} – pitch diameter, σ – taper angle.

To determine the lead angle of the thread helix, the formula is used:

$$\psi = arctan\frac{P}{\pi d_2} \quad (1)$$

Pitch P = 4.233 mm is only possible for threads of small pitch diameters of 27 - 41 mm. Therefore, according to the formula, the largest value $\psi = 2{,}86$ °. Further values of the lead angle are less than 1.87° (pitch diameter from 59.8 mm).

3.2. Trapezoidal Thread Profile According to ISO, ASME and GOST Standards

The main purpose of trapezoidal threads is rotational -translational kinematic pairs with significant axial loads and increased requirements for accuracy of movements. This imposes high requirements for the accuracy of the pitch and flank angle, as well as the strength and wear resistance of the lead screw and nut.

According to GOST [71]: H=1.866P, h_3=0.5P. According to GOST [71] and ISO [73]: flank angle φ=30°, root width k=0.366P, root width along the pitch diameter is 0.5P (Figure 4). According to ASME [72]: root width k=0.3707P, root width along the pitch diameter is also 0.5P (Figure 4).

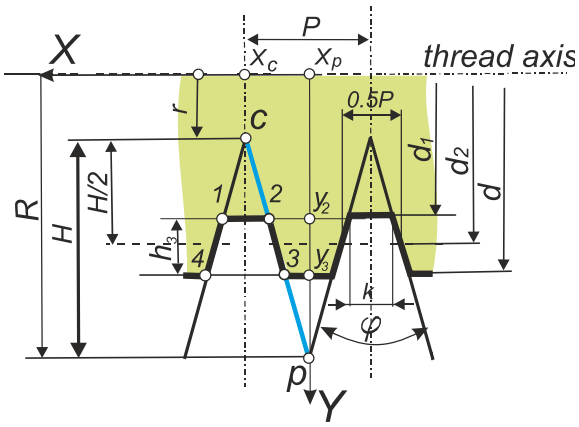

Figure 4. Trapezoidal thread diagram according to GOST 9484-81 [71], ASME [72], ISO [73], "Basic norms of interchangeability. Trapezoidal screw thread. Profiles".

 doi:10.20944/preprints202603.0123.v1

The accuracy of the profile angle φ=29° (Figure 4) of the trapezoidal thread is regulated by the ASME standard [72] and is dependent on the number of threads per inch (Table 2). That is, at Threads/In = 3 (i.e., thread pitch *P*≈8 mm), the accuracy of the flank angle is 22 min.

Table 2. Tolerances on φ/2=14.5 deg flank angle for external and internal Acme screw threads. Fragment of standard [72].

Number of Threads/In	14.5 deg variation	
	deg	min
8	0	35
5	0	27
4	0	25
3	0	22
2	0	18

To determine the largest lead angle of a trapezoidal thread according to the ISO standard, one should select, according to [73], the nominal and pitch diameters of the thread of the smallest value and simultaneously with the largest pitch P. Table 3 contains data that can be used to determine the lead angle of the thread according to formula (3.1).

Table 3. Fragment of the ISO standard on the correspondence of maximum pitches and maximum pitch diameters [73].

Major diameter *d*, mm	Pitch *P* (maximum), mm	Pitch diameter (maximum), mm	Lead angle, ° ψ
16	4	14.00	5,2
24	**8**	**20.00**	**7.26**
32	10	27.00	6.72
44	12	38.00	5.7

Therefore, according to formula (1), the largest lead angle in a trapezoidal thread with a major diameter of 24 mm and a pitch 8 mm is 7.26°.

3.3. Buttress Thread Profile According to the ASME Standard

The main purpose of buttress threads is to withstand high axial loads in one direction, for example, industrial jacks, casing pipes for oil and gas wells. With significant axial loads and increased requirements for accuracy of movements, which imposes high requirements for the accuracy of the pitch and flank angle, as well as the strength and wear resistance of the screw and nut.

According to the ANSI B1.9–1973 standard [74]: H=0.89064P, h=0.6P, r_1=0.07141P, f=0.14532P, F=0.16316P, φ_2=45°, φ_1=7°.

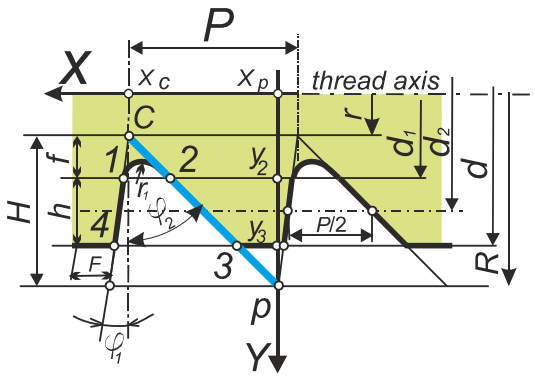

Figure 5. Buttress thread pattern according to ANSI standard [74]. Symbols: d – major diameter, d_1 – minor diameter, d_2 – pitch diameter, P – pitch, H – height of sharp-V thread, h – basic height of thread engagement, r_1 – root radius (theoretical), f – crest truncation, F – crest width.

 doi:10.20944/preprints202603.0123.v1

The accuracy of the flank angles of the thread according to the ANSI standard [74] is represented by the tolerances for angle deviation: 4 min for $\varphi_2 = 45°$ and 5 min for $\varphi_1 = 7°$ (Table 4).

Table 4. Fragment of the ANSI standard on major diameters, pitch and flank angle accuracy [74].

Threads per inch	Pitch, *P*, ≈ mm	Tolerance on flank angles of thread, ± min		Major diameter *d*, inch
		φ_1=7°	φ_2=45°	
16	1.6	5	4	0.5–4
10	2.5	5	4	0.3–16
3	8	5	4	1.5–24
2	12.7	5	4	6-24

Therefore, according to formula (1), the largest lead angle in the buttress thread with a nominal diameter of 1.5′ (≈38 mm) and a pitch of P≈8 mm is 3.83°.

3.4. Comparison of Requirements for the Accuracy of the Thread Profile Angle and the Lead Angle

So nominally the most demanding in terms of accuracy of flank angles is the buttress thread according to the standard [74] with a deviation of 4 min, which is δ=4/(45*60) = 0.15% of the nominal value (Table 4). The trapezoidal thread according to the ASME standard [72] with a deviation of 18 min can be considered less accurate, i.e.: δ=18/(60*14.5)=2%. The least demanding profile accuracy is the tool-joint thread with a deviation of 45 min, which is δ=45/(60*30)=2.5% of the nominal value of the profile angle (Figure 3).

Table 5. Summary of maximum data for buttress, trapezoidal and tool-joint threads in terms of profile angle deviation and lead angle.

Parameters	Tool-joint	Trapezoidal	Buttress
Maximum permissible relative deviation of the profile angle δ	2.5%	2%	0.15%
Maximum thread lead angle ψ (maximum helix lead angle)	2.86°	7.26°	3.83°

It should be noted that buttress threads (P=5.08 mm) as well as triangular tapered threads (P=3.175 mm) are also widely used in the oil and gas industry, for example for connections of well casing pipes. However, despite the high mechanical loads and requirements for corrosion resistance, these threads have quite large diameters (114-508 mm) and therefore, with similar pitch values [75], have a significantly lower lead angle than those used in highly loaded threads [76], for example in powerful jacks.

4. Modern Approaches to Ensuring the Accuracy Form of the Production of Large-Step Threads Made by Turning

4.1. Providing Directrix and Generatrix Lines When Turning Helical Surfaces

All modern threads contain two helical surfaces, with a constant pitch P. Figures 3, 4, 5 show a blue line *cp*, which is the directrix of one of these two helical surfaces. Points 2 and 3 belong to this directrix and are at the same time profile points of the threads: tool-joint, trapezoidal, buttress. Other profile points of these threads 1 and 4 belong to the generatrix of the second helical surface. Since lathes are widely used to manufacture the specified threaded and helical surfaces, considerable attention of manufacturers and researchers is focused on thread cutters and their ability to process difficult-to-machine materials, which include high-strength and corrosion-resistant steels [77]. Of course, such abilities are developed due to the use of modern composite materials for coatings of cutting threaded inserts [78]. At the same time, the actual geometric parameters of the cutters and their movements during thread turning are very influential factors, especially for difficult-to-machine materials [45].

 doi:10.20944/preprints202603.0123.v1

Usually, in the case of threading on a lathe, the cutter is installed in such a way that its cutting edge 4-1-2-3 is aligned with the axial plane of the thread [66,76] (Figure 6). Each point of the cutting edge performs an absolute movement along the trajectory of the helix with a pitch *P*. Points 2 and 3 belong to one helical surface and two boundary helices of this surface: the blue helix with the smallest radius r_2 (point 2) and the red helix with the largest radius R_3 (point 3). All other points forming the helical surface are located between points 2 and 3. Another helical surface is formed by the section of the cutting edge located between points 1 and 4. The absolute movement of the edge points along the helix is ensured by the constant rotational movement of the workpiece around the thread axis *X* and the translational movement of the cutting edge points along the axis *X*. In this case, the module of translational movement $|\overrightarrow{S_t}|$(mm per rotate) is equal to the step size *P* (mm).

Provided that the plane of the cutting edge of the tool is completely aligned with the axial plane of the thread, profiles of the edge and the thread will coincide, and accordingly their profile angles φ will coincide (Figure 7a).

Theoretically, the helical surface is formed by a truncated cone (guide cone), which rotates with a constant circular speed around its axis *X* and moves translationally along this axis. If the cutting edge *3-2* of the cutter lies in the axial plane of the guide cone - the plane X_p-X_c-*c*-*p*, then a regular closed cone is formed in the case of radial feed $\overrightarrow{S_r}$ (Figure 7c). The straight-line generator of the cone *pc* will coincide with the edge *2-3* when the cutter completes the radial feed $\overrightarrow{S_r}$. Such a guide cone provides a theoretically correct closed helicoid (otherwise Archimedes' screw), which defines most fastening threads and all buttress threads and trapezoidal lead screws (Figure 7b). The profile of the guide cone is the same in all axial planes, including *ZX*. The directrix *cp* in the *ZX* plane is described by the equation (Figure 7d):

$$z = -x \cdot ctg\left(\frac{\varphi}{2}\right) \tag{1}$$

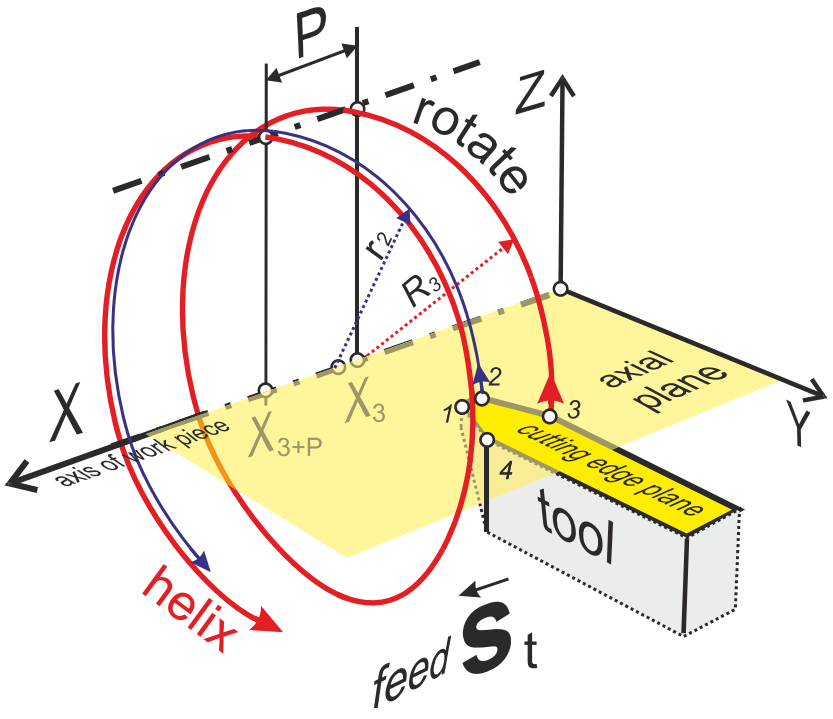

Figure 6. Thread cutter movement diagram: *X* - axis, *P* -pitch, S_t - longitudinal feed per revolution, R_3 - radius of the helix (red) with point *3* on the cutting edge, r_2 - radius of the helix (blue) with point *2* on the cutting edge, X_3, X_{3+P} – coordinates of the points of two adjacent turns of the red helix on the *X* axis; 4, 1, 2, 3 are points that simultaneously belong to the cutting edge of the cutter and the axial plane of the screw *XY* (yellow).

 doi:10.20944/preprints202603.0123.v1

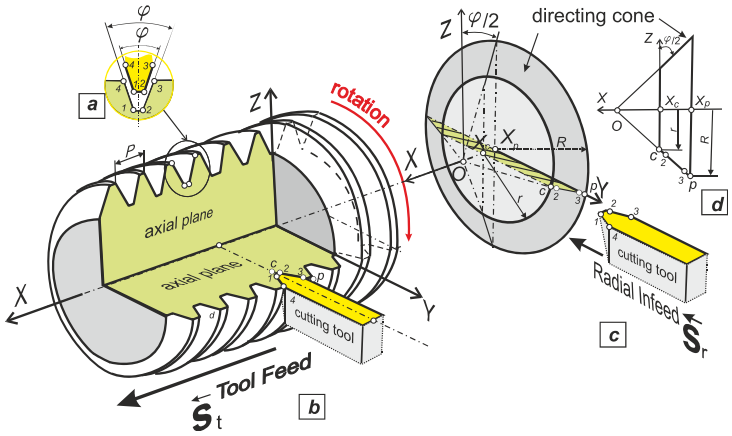

Figure 7. Scheme of forming a trapezoidal thread: **a**) – coincidence of the cutting edge profile (yellow) and the profile of the resulting thread (lime). **b**) – location of the edge of the thread cutter (yellow) in the axial plane of the thread (lime); **c**) – location of the edge of the cutter *2-3* as the generator of the guide cone *cp*. *X* - thread axis, *P* - thread pitch, *R* - radius of the larger base of the guide cone, *r* - radius of the smaller base of the guide cone, X_p, X_c – coordinates of the points of the generating cone of the directrix on the thread axis *X*; φ – thread profile angle, **d**) – location of the projection of the cutting edge *2-3* in the axial plane *ZX*.

4.2. Deviation of the Cutting Edge of the Thread Cutter from the Generating Helical Surface Under the Condition of Using the Cutting Edge Inclination Angle λ

In practice, leading manufacturers of cutting tools often recommend using a special inclination of the cutting insert at an angle λ to the thread axis and supply special shims for this. This inclination angle λ, which is equal to the lead angle, guarantees the same clearance angles of the right and left sides of the insert [66,76] (Figure 8a). This is done to maintain the same operating conditions of the left (*1-4*) and right (*2-3*) cutting edges, which helps to increase the tool life. For versatility, the cutting edge profile of such carbide inserts *4-1-2-3* is made identical to the profile of the corresponding thread (Figure 8b). The diagram of installing the cutter together with the holder with a rotation to an angle λ (Figure 8c) graphically explains the difference compared to installation without rotation to this angle (Figure 7b). However, such an installation is not possible in a conventional lathe toolholder.

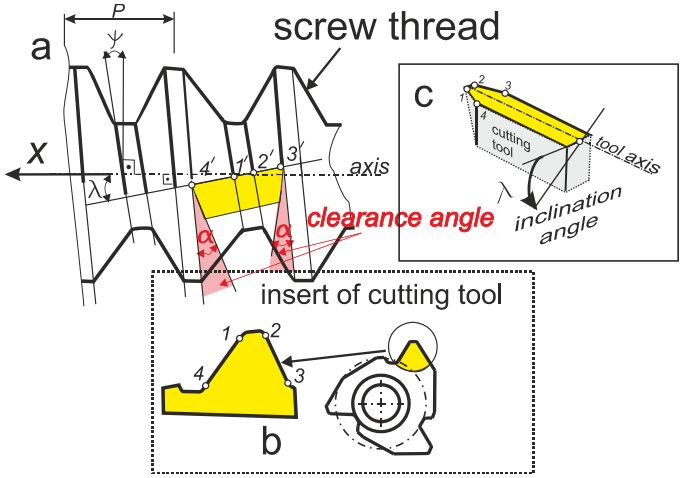

Figure 8. Scheme of installing the cutting insert of the thread cutter: a) at the angle of inclination of the edge λ which corresponds to the lead angle ψ; b) placement of the cutting edge on the threaded insert; c) scheme of turning the thread cutter at an angle λ.

 doi:10.20944/preprints202603.0123.v1

However, it is obvious that the plane where the cutting edge 2-3 is located, in the case of its inclination at an angle λ to the axial plane of the thread (Figure 9a), will not coincide with the generator of the guide cone *cp*. (Figure 8c), which is always located in the axial plane (lime) (Figure 9b).

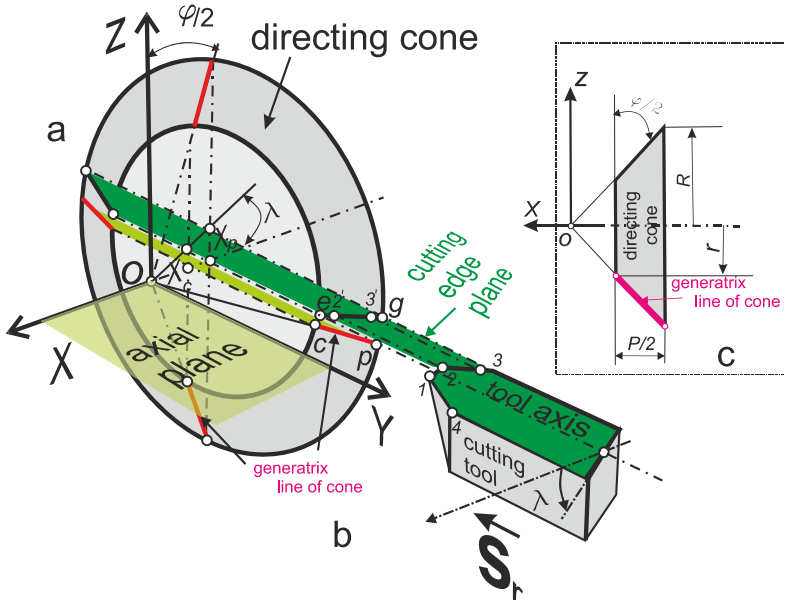

Figure 9. Scheme of installation of the cutting insert of the thread cutter: a) at the angle of inclination of the edge λ, which corresponds to the lead angle ψ; b) placement of the cutting edge on the threaded insert; c) axial projection of the guide cone; *P* is the thread pitch, φ is the profile angle of the thread. Radii *r* and *R* are the parameters of the large and small base of the truncated cone (guide cone).

4.3. Deviation of the Cutting Edge of the Thread Cutter from the Generating Helical Surface Under the Condition of Using the Rake Angle γ

A number of studies suggest the use of a non-zero rake angle for threaded tools [45,54,55,67,68], which significantly expands the capabilities of the cutter when processing various materials (Figure 2, Table 1).

If the value of the rake static angle at the apex of the thread cutter is not zero, but the angle of inclination of the cutting edge has a zero value, then the front plane intersects the generating cone of the thread parallel to its axial plane (Figure 10). The value *k* is the distance from the plane of the section of the guide cone with the plane of the cutting edge of the cutter 2-3-4-1 to the axial plane. *eg* is the line of intersection of the plane of the cutting edge with the guide cone. Obviously, the curve *eg* is not equal to the line *cp*, but it is a real generator of the guide cone and must contain the cutting edge points between points 2 and 3 (Figure 10).

 doi:10.20944/preprints202603.0123.v1

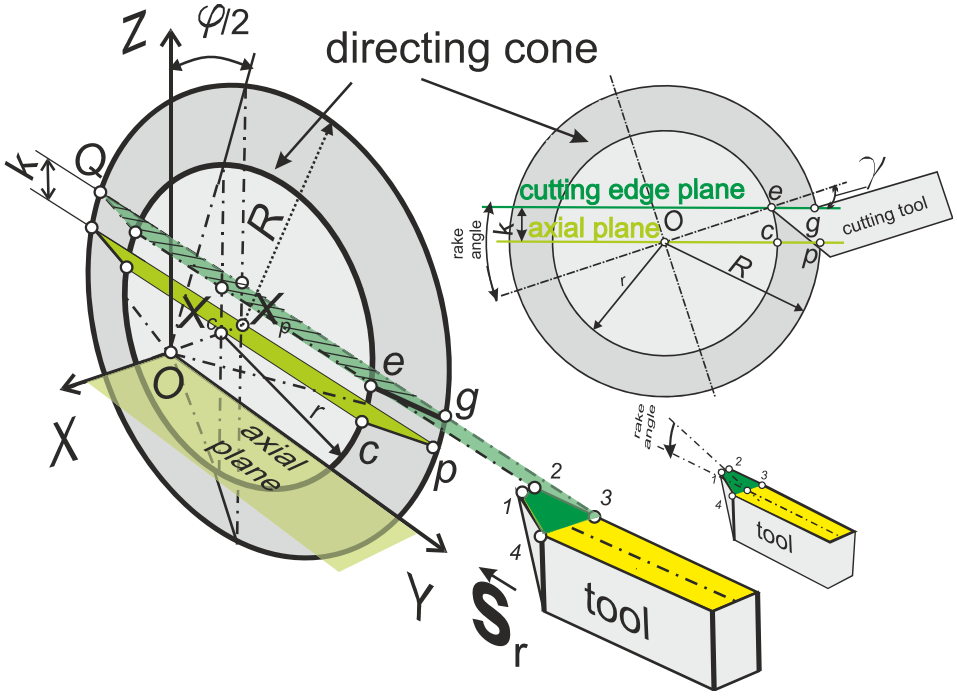

Figure 10. Installation diagram of a thread cutter with a non-zero rake angle, *Spop* – transverse feed.

5. Analytical Calculation of the Points of the Hyperbolic Profile of the Cutting Edge with a Non-Zero Values of the Rake Angle and the Inclination Angle at the Nose

5.1. Analytical Calculation of the Hyperbolic Profile of the Cutting Edge as a Function of the Rake Angle

In fact, when a conical surface is intersected by a plane parallel to the axis of the cone, a hyperbola is formed [79,80]. So, Figure 11 presents a spatial scheme for the formation of a hyperbolic curve *ge*, which should be the shape of the cutting edge of the cutter to create one of the two helical surfaces of the thread with a pitch *P*, a profile angle of the thread φ and the height of the initial triangle *H*.

Therefore, the shaded area in the figures corresponds to the hyperbolic section of the rake plane with the surface of a truncated cone, which is the parallelism surface of a triangular, trapezoidal, or buttress thread [81].

The axes x_2 and x_1 lie, respectively, in the planes of the major and minor bases of the truncated cone.

If the cutting edge is not located in the axial plane of the truncated cone, which is given by the trace f_β (Figure 12), passing through the thread axis, then a cutter with a triangular profile, which should correspond to the thread profile during transverse feed, will reproduce not a triangular, but a hyperbolic thread profile [80].

Therefore, if we consider the section of the thread as the surface of a truncated cone (Figures 11, 12.) with a large radius *R*, a small radius *r* and an angle at the nose, then as a result of the intersection of this cone with the rake plane, which is given by the trace *f*, a hyperbola will be obtained [80].

 doi:10.20944/preprints202603.0123.v1

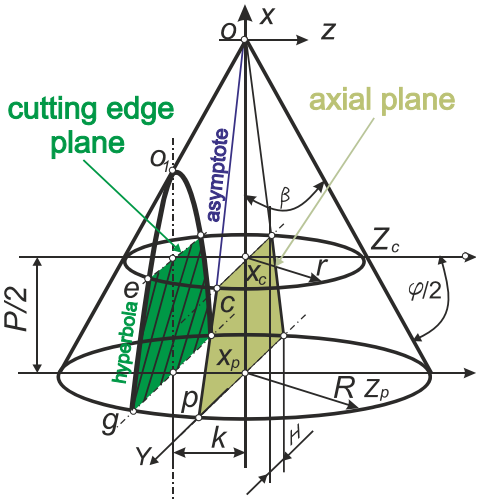

Figure 11. Scheme of obtaining a cross-section of a conical surface and a plane parallel to the axis of the cone. The Y axis is parallel transferred from the vertex of the cone O to the point Xp and then through the point p.

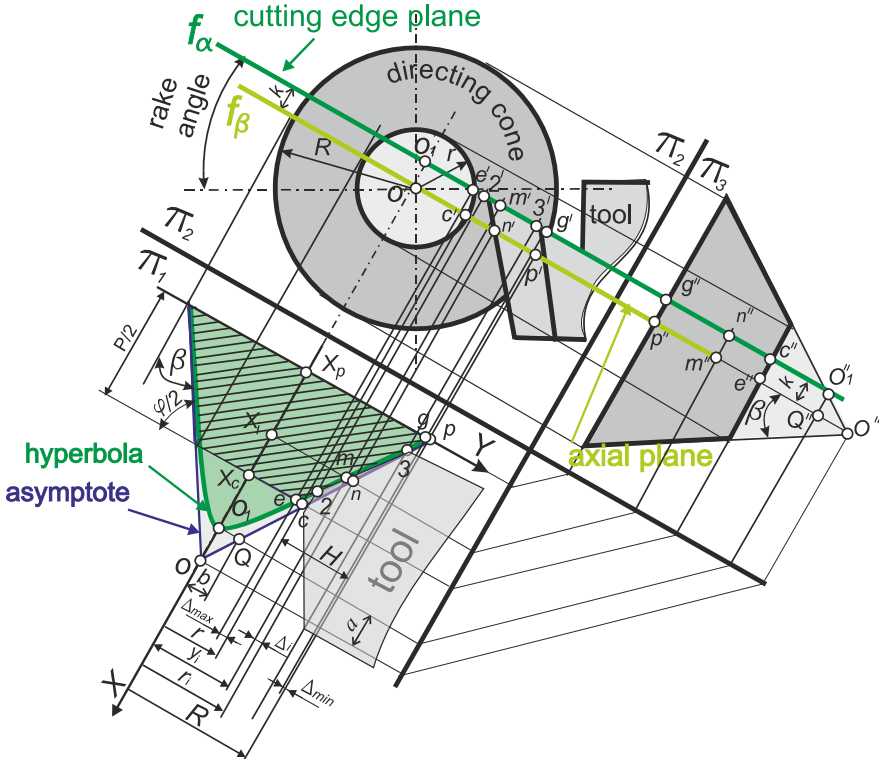

Figure 12. A complex drawing of obtaining a cross-section with a hyperbolic profile when intersecting a cone with a plane that does not pass through its axis.

Hyperbolic section of a cone with axis *OX* and generatrix *Or* with the rake plane marked by the shaded area (Figure 12.). Hyperbola $O_1 emq$ asymptotically approaches the line *Op*. An arbitrarily chosen point *m* at the intersection of the axial plane and the cone corresponds to a point *n* at the intersection of the rake plane and the cone. They have a common coordinate x_n on the *OX* axis. The vertex O_1 of the hyperbola is distant from the vertex of the cone by a distance *a* along the *OX* axis, and the point *Q* is distant by a distance *b* along the *OY* axis.

To calculate the deviation of the hyperbola from the asymptote, depending on the distance from the vertex of the cone *O* along its axis, we use the following formula [80]

 doi:10.20944/preprints202603.0123.v1

$$|mn| = \frac{ab}{x_n + \sqrt{x_n^2 - a^2}} \quad (2)$$

We obtain the dependence of the value of a on the values of the angles β and γ and the radius r. To do this, we determine the value of k, which is marked on the projection plane W (Figure 12). From the right triangle $O''O_1''Q''$:

$$k = |O''Q''|tan\beta$$

Using the projection plane H, we obtain the expression

$$k = a \cdot tan\beta$$

Since the value k is equal to the length of the segment $O_1'O'$ on the projection plane V (Figure 12), then from the right triangle $O_1'O'e$ we have the equation

$$|O_1'O'| = k = |O_1'e|sin\gamma = rsin\gamma$$

Therefore:

$$k = rsin\gamma \quad (3)$$

and accordingly, since $|Q_1'O'|=|Q_1''O'|=k=r\sin\gamma$:

$$a = \frac{r \cdot \sin\gamma}{\mathrm{tg}\,\beta};$$

From the same constructions we obtain the dependence

$$b = a \cdot \mathrm{tg}\,\beta = r \cdot \sin\gamma$$

As a result, we obtain the dependence of the product ab on the values of the angles β and γ and the radius r:

$$ab = \frac{(r \cdot \sin\gamma)^2}{\mathrm{tg}\,\beta} \quad (4)$$

Since point n is taken as an arbitrary point of the cone, and point m is the corresponding point of the hyperbola, then using the concept of an arbitrary i-th point, we will take its coordinates as x_i along the OX axis and r_i along the OY axis. Thus, the asymptote formula will look like this:

$$x_i = \frac{r_i}{\tan\beta} = \frac{r_i}{\tan\left(\frac{\pi}{2} - \frac{\varphi}{2}\right)} = \frac{r_i}{\cot\frac{\varphi}{2}} \quad (5)$$

We replace the notations: $|mn|$ by Δ_i, as well as x_n by x_i and after substituting expressions (4, 5) into formula (2), we obtain the formula

$$\Delta_i = \frac{(r \cdot \sin\gamma)^2/\mathrm{tg}\,\beta}{\frac{r_i}{\mathrm{tg}\,\beta} + \sqrt{\left(\frac{r_i}{\mathrm{tg}\,\beta}\right)^2 - \left(\frac{r \cdot \sin\gamma}{\mathrm{tg}\,\beta}\right)^2}} = \frac{r^2 \cdot \sin^2\gamma}{r_i + \sqrt{r_i^2 - (r \cdot \sin\gamma)^2}} \quad (6)$$

The obtained equation (6) indicates the functional dependence of the magnitude of the displacement of Δ_i the hyperbolic profile of the cutting edge of the thread cutter at an arbitrary i-point on the value of the rake static angle γ at the vertex point e and the radius of the cone at an arbitrary point r_i and the small radius r of the truncated cone.

An arbitrary point on the hyperbola profile can be given in parametric form:

$$y_i = r_i - \Delta_i$$

$$x_i = \frac{r_i}{\cot\frac{\varphi}{2}}$$

So, we describe the profile of the hyperbola as follows:

 doi:10.20944/preprints202603.0123.v1

$$y_i = x_i \cdot ctg\left(\frac{\varphi}{2}\right) - \frac{r^2 \cdot \sin^2\gamma}{x_i \cdot ctg\left(\frac{\varphi}{2}\right) + \sqrt{\left(x_i \cdot ctg\left(\frac{\varphi}{2}\right)\right)^2 - (r \cdot \sin\gamma)^2}} \quad (7)$$

where:

r_i – thread radius at a given point of the profile,

$x_i = \frac{r_i}{\cot\frac{\varphi}{2}}$, – coordinates of the thread profile (2-3) or (1-4) in Figure 4;

φ – profile angle of the thread

5.2. Implementation of Algorithm 1-7 in Python Using the Example of Analyzing the Process of Turning a Trapezoidal Thread of Diameter 24 mm with a Pitch of 8 mm Using a Cutter with a Rake Angle of γ=50°.

The obtained hyperbola functions (equation (7)) and asymptotes (equation (1)) make it possible to make their graphical display and graph-analytical comparison. Figure 13 presents the diagrams of the specified functions made by the authors in Python [82], as well as the diagram of linear interpolation of the hyperbola by the two extreme points *e* and *g*. Only in order to clearly distinguish visually between the hyperbola and its asymptote, the value of the front angle γ=50 ° was used. For example, the diagrams (in Figure 13) were simulated based on the data of the trapezoidal thread according to ISO 2904 and GOST9484-81 with a nominal diameter of 24 mm and a pitch of 8 mm (Figure 4). The diagram in Figure 13, for the sake of clarity of its perception, has been copied into Figure 14, where it is commented on with data and terms from Figures 11 and 12. The calculations of the geometric parameters of a trapezoidal thread with a nominal diameter of 24 mm and a pitch of 8 mm, necessary for constructing the diagrams, are presented in Table 6.

Table 6. Summary of geometric and design data for trapezoidal threads with a nominal diameter of 24 mm and a pitch of 8 mm according to ISO 2904 [73] and GOST9484-81 [71].

Symbol	Parameter name	Formula for determining	Value
	Data according to standards		
d	Major diameter		24.00mm
d_2	Pitch diameter		20 mm
P	Pitch		8 mm
d_3	Minor diameter		15.00 mm
H	Height of the fundamental triangle	H=1.866P	14.928 mm
H_1	Height of the profile	H_1=0.5 P	7.464 mm
a_c	Clearance		0.5 mm
h_3	External thread profile height	h_3=H_1+a_c	4.5 mm
	Calculated data		
R	Major radius of the guide cone	R= d_2/2+H/2	17.464 mm
r	Minor radius of the guide cone	r=d_2/2-H/2	2.536 mm
|1-2|	Shelf length	|1-2|=0.366P – 2a_c · $tg(\varphi/2)$	2.66 mm
	Formulas for calculating the profile angle of the cutting edge φ_2		
X2	X-coordinate of point 2	(d/2 - h_3)ctg(φ/2),	
X3	X-coordinate of point 3	(d/2)ctg(φ/2),	
Y2	Y-coordinate of point 2	Y_3 -$h3$	
Y3	Y-coordinate of point 3	d/2	
	Geometry of the cutting part of the cutter		
γ	Rake angle of the cutter		50°

 doi:10.20944/preprints202603.0123.v1

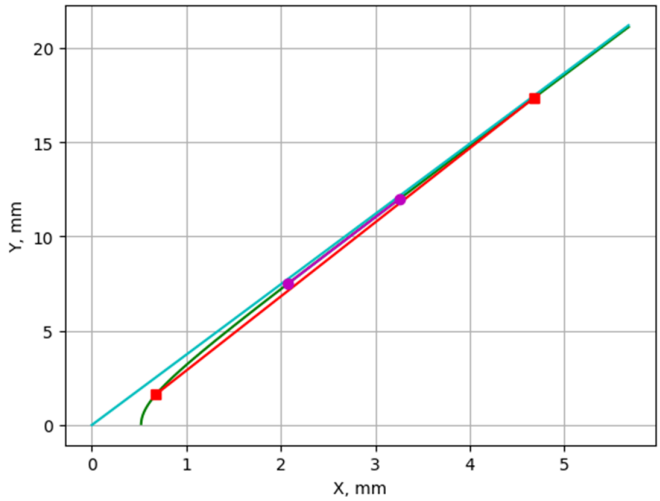

Figure 13. Diagram of the straight section of the trapezoidal thread profile according to ISO 2904/ GOST9484-81 with a nominal diameter of 24 mm, a pitch of 8 mm (blue line), a hyperbolic profile of the cutting edge of the cutter as a function of the rake angle γ=50° (green curve), and a linear interpolation of the hyperbola by the two points (red line, magenta line).

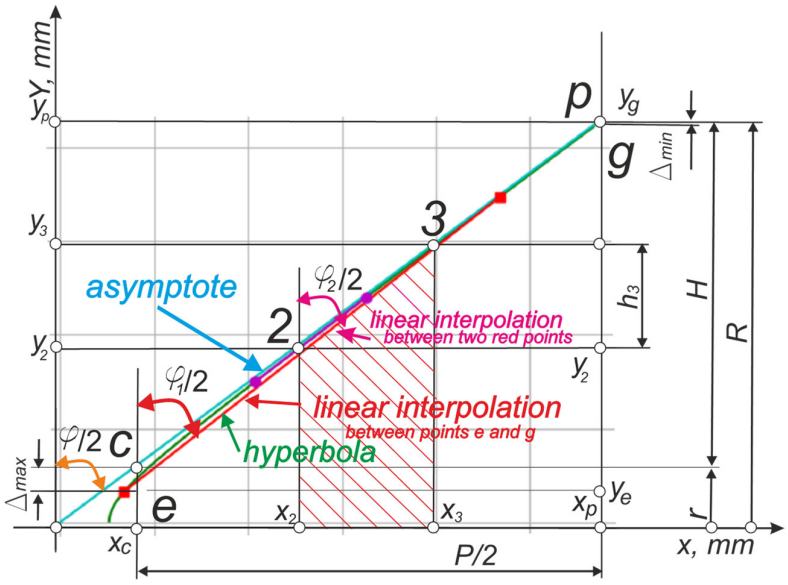

Figure 14. Diagrams with comments: straight-sided section of the profile of a trapezoidal thread 2-3 according to ISO 2904 [73] and GOST 9484-81 [71], with a nominal diameter of 24, a pitch of 8 mm (orange straight line) and a hyperbolic profile of the cutting edge of the cutter as a function of the rake angle γ=50° (section on the blue curve between points with coordinates x_2 and x_3).

5.3. Analysis of the Convexity (Concavity) Arrow of a Hyperbola and Its Maximum and Minimum Deviations from the Asymptote

Visual scaling of the thread profile and cutting edge of the thread cutter in Figure 15 was performed to determine:

the values of the maximum Δmax and minimum Δmin deviations of the simulated hyperbolic curve *emg* (which includes the model of the cutting edge profile of the thread cutter) from the asymptote *sr* (the given cutting edge profile, which is equal to the profile of the given thread).

 doi:10.20944/preprints202603.0123.v1

the angles of the standard cutting edge profile (φ/2) (Figure 15a, Figure 14) and the angle of of the interpolation line *eg* (φ1/2) (Figure 15a, Figure 14).

deviation values $|Am| = si$ of given points *m* of the obtained hyperbolic profile of the cutting edge of the thread cutter *emg* from points *A* of the interpolation line *eg*.

profile angle φ2/2 of the simulated cutting edge intended for forming the straight-sided section of the thread profile 2-3, which belongs to the asymptote (Figure 15b, Figure 14).

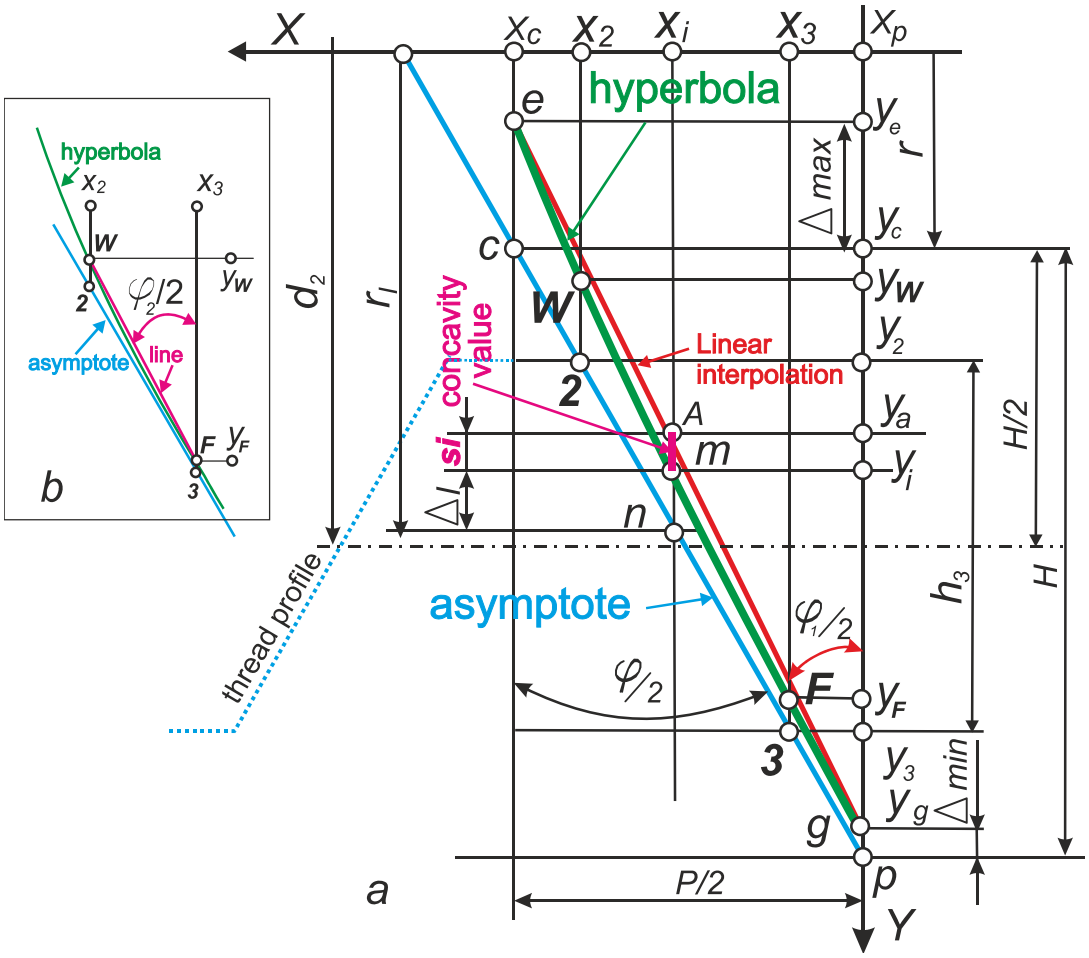

Figure 15. Scheme for determining the deviation (concavity) value *si* of an arbitrary point *n* of the hyperbola, as well as for determining the plane of the cutting edge constructed as a result of the section of the guide cone, which is placed at an angle γ to the axial plane of the thread.

5.3.1. The Formulas for Calculating the Maximum Deviations Δmax and Minimum Deviations Δmin

Deviations of the simulated hyperbolic curve *emg* (which includes the model of the cutting edge profile) from the asymptote *cp* (a given cutting edge profile equal to the profile of the given thread) can be determined based on formula (6):

$$\Delta_i = \frac{r^2 \cdot \sin^2 \gamma}{r_i + \sqrt{r_i^2 - (r \cdot \sin \gamma)^2}}$$

According to Figure 12 and Figure 15, to determine Δmax, the following substitution should be made $r_i = r$:

 doi:10.20944/preprints202603.0123.v1

$$\Delta_{max}=\frac{r^2\cdot\sin^2\gamma}{r+\sqrt{(r)^2-(r\cdot\sin\gamma)^2}}=r-\frac{r\cdot\sin^2\gamma}{1+cos\gamma} \quad (8)$$

According to Figure 12 and Figure 15, to determine Δmin, the substitution should be made r_i=R:

$$\Delta_{min}=R-\frac{r^2\cdot\sin^2\gamma}{R+\sqrt{R^2-(r\cdot\sin\gamma)^2}} \quad (9)$$

5.3.2. Determination of the Angles of the Interpolation Lines eg and wf.

Proflie angles $\frac{\varphi}{2},\frac{\varphi 1}{2},\varphi 2/2$ can be determined by Figure 15 and formulas in Table 7:

Table 7. Summary of angle calculation formulas φ, φ_1, φ_2.

Symbol	Name	Formula	Comments
φ/2	Flank angle (half-profile angle)	$\frac{\varphi}{2}=arctan\frac{x_3-x_2}{y_3-y_2}$ (10)	15° according to standards ISO 2904 [73] and GOST 9484-81 [71]
$\varphi_1/2$	The angle of the interpolation line between two points g and e	$\frac{\varphi_1}{2}=arctan\frac{x_p-x_c}{y_g-y_e}$ (11)	$x_c=r\tan\frac{\varphi}{2}$ $x_p=R\tan\frac{\varphi}{2}$ $y_c=r$ $y_e=r-\Delta_{max}$ $y_p=R$ $y_g=R-\Delta_{min}$
$\varphi_2/2$	Cutting edge profile angle	$\frac{\varphi_2}{2}=arctan\frac{x_3-x_2}{y_F-y_w}$ (12)	$x_3=\left(r+\frac{H}{2}+\frac{h_3}{2}\right)\tan\frac{\varphi}{2}$ $x_2=\left(r+\frac{H}{2}-\frac{h_3}{2}\right)\tan\frac{\varphi}{2}$ y_f determined by *(7)* for $x_i=x_3$ y_w в determined by *(7)* for $x_i=x_2$

5.3.3. Definition of the Deviation (Concavity Value) of Hyperbola emg by Software-Analytical Method

For the analytical definition of the deviation (concavity value) of the hyperbola *emg*, it is necessary to find the maximum distance between the points of the hyperbola and the corresponding points of the interpolation line $|Am|=si$. (Figure 15), that is, find the maximum value of the difference between Y coordinates:

$$|s_i|=y_{int}-y \quad (13)$$

where:

y is determined by formula (7) for a given array of points with coordinates x_i for i={x_c, … x_p};

y_{int} – for the same array of points i={x_c,… x_p} using Figure 16 we determine using the method [80] the interpolation line *eg* , i.e. we create a line through the point e(x_c,y_e) and we determine the point g (x_p,y_g) by the formula:

$$y_{int}=\frac{(x-x_c)(y_g-y_e)}{(x_p-x_c)}+y_e \quad (14)$$

where formulas for calculating point coordinates x_c,x_p,y_g,y_e are listed in Table 7.

 doi:10.20944/preprints202603.0123.v1

Using Python based on the algorithm built on the basis of formulas (7), (13-14), an application [82] was created to determine the maximum possible distance *si* :

Table 8. Data and results of the calculation of the boom s_i convexity of hyperbola *emg*.

Thread diameter, mm	Thread pitch	The value of the rake angle γ, °	si, mm
24	8	50	0.01
24	8	20	0.002
24	8	10	0.00056

5.3.4. Definition of the Arrow of Convexity (Concavity Value) of the Hyperbola Section emg, Which Corresponds to the Cutting Edge of WF by the Program in Python

Based on Figure 15 and using the Python, an application [82] was developed that allows calculating the distances between the hyperbola and the straight interpolation line drawn through the points W, F of the cutting edge of the modeled cutter for machining the threaded part 2-3. The program allows for a rectilinear approximation of the hyperbola section *emg.*

Figure 16 shows the distribution graphs of these distances: between the hyperbola and the interpolation line *WF* (upper curves), between the hyperbola and the approximation line (lower curves).

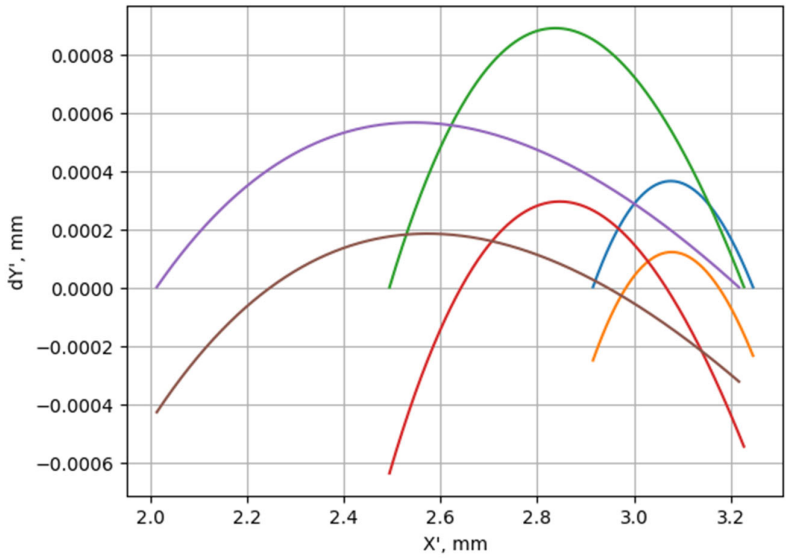

Figure 16. Distances from the interpolation line *WF (*upper curves*)* and the approximation line *(*lower curves*)* to the corresponding points of the hyperbolic curve *WF* modeled according to formula (7) intended for forming the cutting edge *2-3* of a tool with a rake angle γ=10° for *P*=2 mm (right), 5 mm (middle), 8 mm (left).

5.4. Analytical Calculation of Linear Interpolation at the Two Extreme Points of the Hyperbolic Profile of the Cutting Edge as a Function of the Rake Angle at the Nose and the Inclination Angle Simultaneously

To ensure high productivity of the thread cutter, the cutting edge plane (i.e., the rake plane) should be placed not only at the rake angle γ, but also at the cutting edge inclination angle λ, as recommended by tool manufacturers [66,76].

From the point of view of the well-known theory of conic sections [80], a hyperbola will be obtained under the conditions:

- if we cross the conical surface with a plane that is parallel to the axis of the cone. In Figure 17a , the plane *f* intersects the conical surface at a distance *k* from the axis and is located parallel to the axis. The value of *k* depends on the value of the rake angle according to formula (3);

 doi:10.20944/preprints202603.0123.v1

- if we cross the conical surface at an angle λ whose value is greater than 0° and less than the angle at the vertex of the cone β (Figure 17b);
- if we cross the conical surface with a plane parallel to the generator of the cone, we will obtain a parabolic profile (Figure 17c).

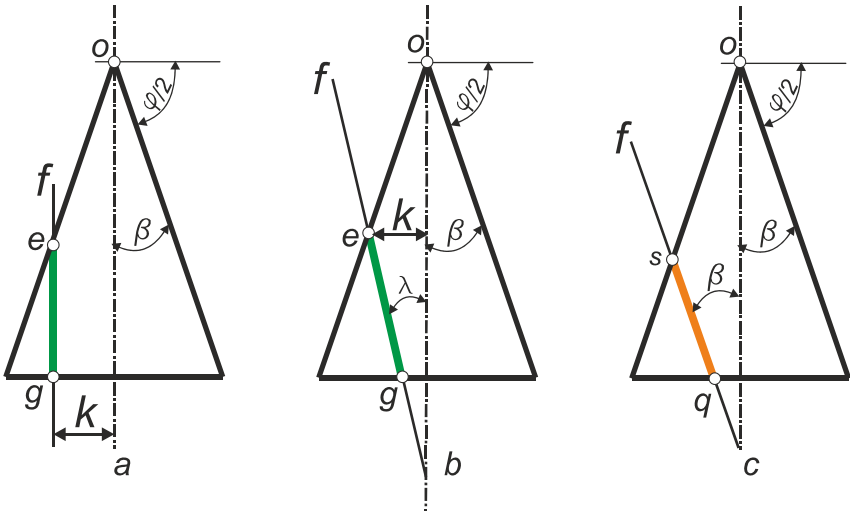

Figure 17. Schemes illustrating the origin of the hyperbolic and parabolic cross-section depending on the position of the rake plane: *f* – frontal trace of the rake plane, λ – inclination angle of the rake plane to the axis of the conical surface, β – half angle at the apex of the cone.

That is, provided that $0° < \lambda < (\frac{\pi}{2} - \frac{\varphi}{2})°$ the cross-section of this triangular thread and the plane of the rake surface with a double slope is hyperbolic.

It is possible to determine the coordinates of the extreme points of the intersection of the plane ***uAv*** with the surface of a truncated cone with height $\pi/2$ as the lines of intersection of the hyperbola with circles with radii *r* and *R* (Figure 18).

Therefore, the indicated shaded region is bounded by a hyperbolic curve formed by the intersection of the rake flat surface of the thread cutter, whose parameters $\lambda \neq 0$ and $\gamma \neq 0$ the parallelogram surface of the triangular thread, i.e., with a cone of height *h* and an angle at the vertex β.

It is possible to determine the coordinates of the extreme points of the intersection of the plane ***uAv*** with the surface of a truncated cone with height $\pi/2$ as the lines of intersection of a hyperbola with circles of radii *r* and *R* (Figure 18).

In the plane of a circle with radius *r* (plane $y0x_2$) – coordinates on the *v* axis:

$$v_{min} = \sqrt{r^2 - k^2} \tag{15}$$

In the same plane we have the minimum value of the coordinate along the *u* axis:

$$u_{\min} = 0$$

In the plane of a circle with radius *R* (the plane that is parallel to $y0_1x_1$ and contains the x_2 axis) – the coordinates on the *v* axis are:

$$v_{max} = \sqrt{R^2 - \left(k - \frac{P}{2}tan\,\lambda\right)^2} \tag{16}$$

where:

according to the formula (3) $k = r\,sin\,\gamma$

In the same plane we have the maximum value of the coordinate along the *u* axis:

 doi:10.20944/preprints202603.0123.v1

$$u_{max} = \frac{P}{2\cos\lambda} \tag{17}$$

Determining the profile angle of the cutting edge of the cutter (according to the diagram in Figure 19):

$$\varphi_2 = 2\,arctan\left(\frac{u_{max}}{(v_{max} - v_{min})}\right) \tag{18}$$

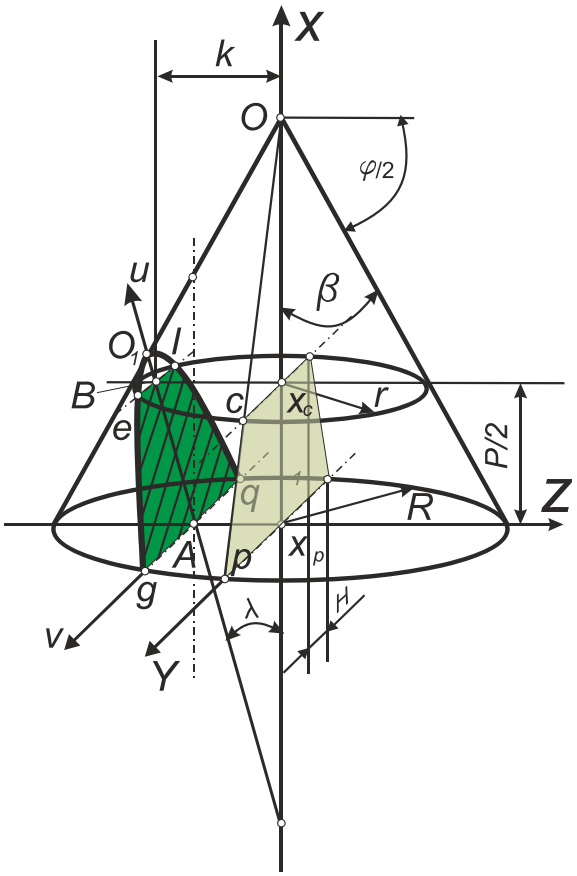

Figure 18. Scheme for obtaining a cross-section of a conical surface and a plane inclined to the axis of the cone at an angleλ.

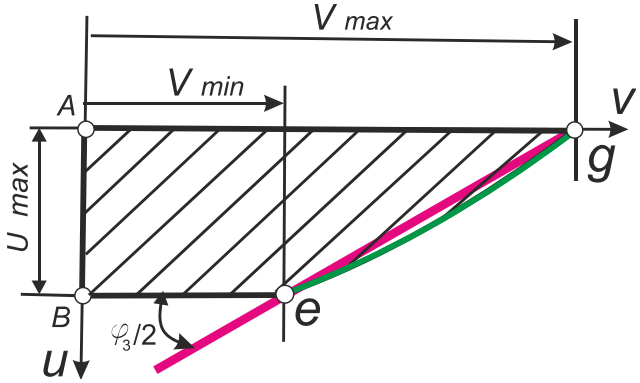

Figure 19. Scheme for determining the profile angle φ_2 of the simulated lateral straight cutting edge of the cutter as a function of its geometric parameters γ and λ.

 doi:10.20944/preprints202603.0123.v1

6. Results of Calculation and Modeling of the Interpolated Hyperbolic Profile of the Cutting Edge of the Cutter with a Non-Zero Value of the Front Angle and the Angle of Inclination of the Cutting Edge at the Apex of Its Blade

6.1. Results of Calculation of the Value of the Profile Angles of the Cutting Edge of the Modeled Thread Cutters with Interpolated Cutting Edges According to Formulas (12) and (18) (Table 9)

As can be seen from the table, increasing the thread pitch to 8 mm requires a significant change in the angle λ , which in turn significantly requires a change in the profile angle φ of the cutting edge of the cutter to a value of 30.141°, in contrast to 29.969° when not using the inclination angle λ=7 °.

Table 9. Examples of calculating the profile angle of the cutting edge φ_2 of the cutter ⌀2 for a trapezoidal thread with a nominal diameter of 24 mm.

Thread pitch P, mm	Rake angle of the tool γ, °	Profile angle of the cutting edge (taking into account the influence of only the angle γ) (according to equation (12))	Cutting edge inclination λ,°	Profile angle of the cutting edge (taking into account the influence of the angle γ and cutting edge inclination λ,°) (according to equation (18))
8	10	29.969	7	30.141
5	10	29.857	4	29.865
2	10	29.694	2	29.671

6.2. Model of the Cutting Edge Profile with Interpolated Straight Sides

Based on the obtained values φ_3 (18) , as well as Δmax (8) and Δmin (9), it is possible to construct a high-precision profile of the initial theoretical triangle of the thread cutter (Figure 20).

The values *H, h3, P* are in accordance with the standards [71–74].

The value *flat1*=|1-2|·cosλ, where |1-2| is determined based on standards [71–74].

The value δ is determined as a result of the graphical construction of the shelf *TS* , the length of which is equal to *flat1*.

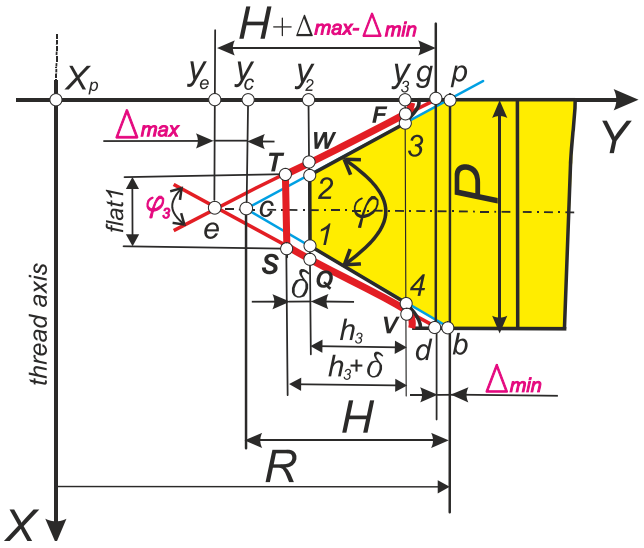

Figure 20. Scheme for constructing the complete profile of the cutting edge of a cutter for threading.

 doi:10.20944/preprints202603.0123.v1

7. Discussions

The data in Table 8 actually indicate that the convexity of the simulated cutting edge of 0.002 mm is technologically imperceptible at the value of the rake angle γ=20 °, and the convexity of 0.00056 mm at the value of the rake angle γ=10 ° is practically unreproducible. Therefore, taking into account these data, as well as the recommendations for the range of the rake angle within 0 ... 25 °, the authors believe that the modernization of the cutting edge profile of the threading cutter should be ensured by interpolation at two extreme points. This formed the basis for calculating the linear interpolation at two extreme points of the hyperbolic profile of the cutter cutting edge as a function of the rake angle at its apex and the angle of inclination of the cutting edge simultaneously, i.e. the application of formulas (15)-(18).

8. Conclusions

Turning cutting tools for the production of threaded parts from critical materials, especially parts with high quality (oil and gas too joints with triangle threads and buttress threads profile, jack screws and lead screws with a trapezoidal thread) require, to ensure durability, non-zero values of the geometric parameters: the rake angle γ and the cutting edge inclination λ, which needs their high-precision profiling.

The most technologically advanced approach is to replace the curvilinear hyperbolic profile, which is theoretically responsible for the non-zero value of the rake angle γ and the edge inclination angle λ by straight profile based on interpolation beyond the two extreme points of the hyperbolic profile.

In the case of the need to manufacture large-pitch threads, there is a need to significantly increase the inclination angle to λ=7°, which leads to the need for a significant change in the cutting edge profile, which consists in changing the profile angle and the length of the cutting part of the tool.

The analytical approach to modelling the profile of a high-precision thread is based on functions, where the arguments are the thread parameters: diameter, pitch, as well as the geometric parameters of the cutter: rake angle and cutting edge inclination angle.

Author Contributions: Conceptualization, C.B., O.O. and V.K.; methodology, C.B. and O.O.; software, O.O. and V.K.; validation, V.K., Y.K. and S.B.; formal analysis, O.O. and Y.K.; investigation, C.B. and O.O.; resources, L.S. and Y.K; data curation, L.S. and S.B.; writing—original draft preparation, O.O. and V.K.; writing—review and editing, P.D., V.K. and S.B.; visualization, Y.K. and P.D.; supervision, L.S. and P.D.; project administration, O.O.; funding acquisition, O.O. All authors have read and agreed to the published version of the manuscript.

Funding: This research was funded by the Ministry of Education and Science of Ukraine, grant

number PK 0124U000654.

Data Availability Statement: Data are contained within the article.

Conflicts of Interest: The authors declare no conflicts of interest.

References

1. Nascimento, A.; Mantegazini, D.Z.; Mathias, M.H.; Reich, M.; Hunt, J.D. O&G, Geothermal Systems, and Natural Hydrogen Well Drilling: Market Analysis and Review. *Energies* **2025**, 18, 1608. https://doi.org/10.3390/en18071608
2. Sharmin, T.; Rodoshi Khan, N.; Md Saleh Akram; Ehsan, M. A State-of-the-Art Review on Geothermal Energy Extraction, Utilization, and Improvement Strategies: Conventional, Hybridized, and Enhanced Geothermal Systems. *International Journal of Thermofluids* **2023**, 18, 100323, https://doi.org/10.1016/j.ijft.2023.100323
3. Matiyiv, K.; Klymchuk, I.; Arkhypova, L.; Korchemlyuk, M. Surface water quality of the prut river basin in a tourist destination. *Ecological Engineering & Environmental Technology*, **2022**, 23(4), 107–114. doi: 10.12912/27197050/150311.

 doi:10.20944/preprints202603.0123.v1

4. Kravchynskyi, R.L.; Khilchevskyi, V.K.; Korchemluk, M.V.; Arkhypova, L.M.; Plichko, L.V. Criteria for identification of landslides in the upper Prut River basin on satellite images. Geoinformatics. 11-14 May 2021, pp.1-6. doi: 10.3997/2214-4609.20215521003.
5. Prykhodko, M.; Arkhypova, L.; Fomenko, N.; Syrovets, S.; Varianichko, V.; Osypov, D. Economic value of ecosystem services in the landscapes of Ukraine. 17th International Conference Monitoring of Geological Processes and Ecological Condition of the Environment. Nov. 2023. pp.1-5. https://doi.org/10.3997/2214-4609.2023520221
6. Glibovytska, N.; Rashevska, H.; Arkhypova, L.; Adamenko, Y.; Orfanova, M. Impact of electric power facilities on natural phytocenotic diversity. *Ukrainian Journal of Forest and Wood Science*, **2024**, 15(2), 8–22. doi: 10.31548/forest/2.2024.08.
7. Wu, B.; Zhang, K.; Meng, G.; Suo, X. Optimization of Recharge Schemes for Deep Excavation in the Confined Water-Rich Stratum. *Sustainability*, **2023**, 15, 5432. https://doi.org/10.3390/su15065432
8. Vlasiy, O.; Mazurenko, V.; Ropyak, L.; Rogal, O. Improving the aluminum drill pipes stability by optimizing the shape of protector thickening. *Eastern-European Journal of Enterprise Technologies* **2017**, 1, 25–31. https://doi.org/10.15587/1729-4061.2017.65718
9. Qin, Jg.; Feng, Zy.; Wang, M.; et al. Research on the design and performance of drill pipe joints based on fracture mechanics methods. *Sci Rep* **2025**, 15, 22790. https://doi.org/10.1038/s41598-025-05587-9
10. Kopei, V.; Onysko, O.; Panchuk, V.; Pituley, L.; Schuliar, I. Influence of Working Height of a Thread Profile on Quality Indicators of the Drill-String Tool-Joint. Conference Advanced Manufacturing Processes III, 7-10 Sep. «InterPartner» 2021. LNME, Odesa. pp.395–404. doi: 10.1007/978-3-030-91327-4_39
11. Prysyazhnyuk, P.; Molenda, M.; Romanyshyn, T.; Ropyak, L.; Romanyshyn, L.; Vytvytskyi, V. Development of a hardbanding material for drill pipes based on high-manganese steel reinforced with complex carbides. *Acta Montanistica Slovaca* **2022**, 27, 685–696. https://doi.org/10.46544/AMS.v27i3.09
12. Kopei, V.; Onysko, O.; Odosii, Z.; Pituley, L.; Goroshko, A. Investigation of the influence of tapered thread profile accuracy on the mechanical stress, fatigue safety factor and contact pressure. In *Lecture Notes in Networks and Systems*, New Technologies, Development and Application IV. NT 2021; Karabegović I. Eds.; Springer: Cham, Switzerland, 2021; Volume 233, pp. 177-185 https://doi.org/10.1007/978-3-030-75275-0_21
13. Shatskyi, I.; Ropyak, L.; Velychkovych, A. Model of contact interaction in threaded joint equipped with spring-loaded collet. *Engineering Solid Mechanics* **2020**, 8, 301–312. https://doi.org/10.5267/j.esm.2020.4.002
14. Croccolo, D.; De Agostinis, M.; Fini, S.; Mele, M.; Olmi, G.; Scapecchi, C.; Tariq, M.H.B. Failure of Threaded Connections: A Literature Review. *Machines* **2023**, 11, 212. https://doi.org/10.3390/machines11020212
15. Ropyak, L.Y.; Vytvytskyi, V.S.; Velychkovych, A.S.; Pryhorovska, T.O.; Shovkoplias, M.V. Study on grinding mode effect on external conical thread quality. *IOP Conf. Ser. Mater. Sci. Eng*. **2021**, 1018, 012014. https://doi.org/10.1088/1757-899X/1018/1/012014
16. Chudyk, I.; Raiter, P.; Grydzhuk, Ya.; Yurych, L. Mathematical model of oscillations of a drill tool with a drill bit of cutting-scraping type. *Naukovyi Visnyk Natsionalnoho Hirnychoho Universytetu* **2020**, 52–57. https://doi.org/10.33271/nvngu/2020-1/052
17. Akl, W.; Alsupie, H.; Sassi, S.; Baz, A.M. Vibration of Periodic Drill-Strings with Local Sources of Resonance. *Vibration* **2021**, 4, 586-601. https://doi.org/10.3390/vibration4030034
18. Landar, S.; Velychkovych, A.; Ropyak, L.; Andrusyak, A. A Method for Applying the Use of a Smart 4 Controller for the Assessment of Drill String Bottom-Part Vibrations and Shock Loads. *Vibration* **2024**, 7, 802–828. https://doi.org/10.3390/vibration7030043
19. Liu, W.; Yang, F.; Zhu, X.; Chen, X. Stick-slip vibration behaviors of BHA and its control method in highly-deviated wells. *Alex. Eng. J.* **2022**, 61, 9757–9767. https://doi.org/10.1016/j.aej.2022.01.039
20. Bembenek, M.; Grydzhuk, Y.; Gajdzik, B.; Ropyak, L.; Pashechko, M.; Slabyi, O.; Al-Tanakchi, A.; Pryhorovska, T. An Analytical–Numerical Model for Determining "Drill String–Wellbore" Frictional Interaction Forces. *Energies* **2024**, 17, 301. https://doi.org/10.3390/en17020301
21. Velichkovich, A.S.; Popadyuk, I.I.; Shopa, V.M. Experimental study of shell flexible component for drilling vibration damping devices. *Chem. Pet. Eng.* **2011**, 46, 518–524. https://doi.org/10.1007/s10556-011-9370-9
22. Li, Fang Po. Surface Galling Mechanism Analysis of Rotary Shouldered Thread Connection. *Materials Science Forum* **2020**, 993, 1286–1292. https://doi.org/10.4028/www.scientific.net/msf.993.1286

 doi:10.20944/preprints202603.0123.v1

23. Velychkovych, A.; Mykhailiuk, V.; Andrusyak, A. Numerical Model for Studying the Properties of a New Friction Damper Developed Based on the Shell with a Helical Cut. *Appl. Mech.* **2025**, 6, 1. https://doi.org/10.3390/applmech6010001
24. Landar, S.; Velychkovych, A.; Mykhailiuk, V. Numerical and analytical models of the mechanism of torque and axial load transmission in a shock absorber for drilling oil, gas and geothermal wells. *Engineering Solid Mechanics* **2024**, 12(3), 207–220. https://doi.org/10.5267/j.esm.2024.3.002
25. Shatskyi, I.; Velychkovych, A. Analytical Model of Structural Damping in Friction Module of Shell Shock Absorber Connected to Spring. Shock. Vib. 2023, 2023, 4140583. https://doi.org/10.1155/2023/4140583
26. Velychkovych, A.; Petryk, I.; Ropyak, L. Analytical study of operational properties of a plate shock absorber of a sucker-rod string. *Shock and Vibration* **2020**,. 3292713. https://doi.org/10.1155/2020/3292713
27. Zheng, Y.; Zhang, Y.; Sun, B.; Zhang, B.; Zhang, S.; Jin, S.; Xiao, Z.; Chu, S.; Jing, Y.; Zhang, Z. Corrosion Behavior and Mechanical Performance of Drill Pipe Steel in a CO 2 /H 2 S-Drilling-Fluid Environment. *Processes* **2024**, 12, 502. https://doi.org/10.3390/pr12030502
28. Li, L.; Lian, Z.; Zhou, C. Failure Analysis of Drill Pipe during Working Process in a Deep Well: A Case Study. *Processes* **2022**, 10, 1765. https://doi.org/10.3390/pr10091765
29. Wang, Y.; Qian, C.; Kong, L.; Zhou, Q.; Gong, J. Design Optimization for the Thin-Walled Joint Thread of a Coring Tool Used for Deep Boreholes. *Appl. Sci.* **2020**, 10, 2669. https://doi.org/10.3390/app10082669
30. Pryhorovska, T.O.; Ropyak, L. Machining Error Influnce on Stress State of Conical Thread Joint Details. 2019 IEEE 8th International Conference on Advanced Optoelectronics and Lasers (CAOL) 2019, pp.493-497. https://doi.org/10.1109/CAOL46282.2019.9019544
31. Tutko, T.; Dubei, O.; Ropyak, L.; Vytvytskyi, V. Determination of Radial Displacement Coefficient for Designing of Thread Joint of Thin-Walled Shells. In Conference Advances in Design, Simulation and Manufacturing IV. DSMIE 2021.Lecture Notes in Mechanical Engineering 2021; pp. 153–162. https://doi.org/10.1007/978-3-030-77719-7_16
32. Kim, B.; Yoon, J.-Y. Structural Optimization of a Circular Symmetric Threaded Connection System Based on the Effect of the Upper Stabbing Flank Corner Radius. *Symmetry* **2022**, 14, 2553. https://doi.org/10.3390/sym14122553
33. Shats'kyi, I.P. Closure of a longitudinal crack in a shallow cylindrical shell in bending. *Mater. Sci.* **2005**, 41, 186–191. https://doi.org/10.1007/s11003-005-0149-z
34. Shats'kyi, I.P.; Makoviichuk, M.V. Analysis of the limiting state of cylindrical shells with cracks with regard for the contact of crack lips. *Strength Mater.* **2009**, 41, 560–565. https://doi.org/10.1007/s11223-009-9166-8
35. Zhang, J.-Y.; Peng, C.; Fu, J.-H.; Cao, Q.; Su, Y.; Pang, J.-Y.; Yu, Z.-Q. Analysis of mechanical strengths of extreme line casing joint considering geometric, material, and contact nonlinearities. Petroleum Science 2024, 21, 1992–2004. https://doi.org/10.1016/j.petsci.2024.02.014
36. Shats'kyi, I.P.; Makoviichuk, M.V. Contact interaction of crack lips in shallow shells in bending with tension. *Mater. Sci.* **2005**, 41, 486–494. https://doi.org/10.1007/s11003-006-0006-8
37. Shatskii, I.P.; Makoviichuk, N.V. Effect of closure of collinear cracks on the stress-strain state and the limiting equilibrium of bent shallow shells. *J. Appl. Mech. Tech. Phys.* **2011**, 52, 464–470. https://doi.org/10.1134/S0021894411030175
38. Karpus, V.E.; Ivanov, V.A. Locating accuracy of shafts in V-blocks. *Russian Engineering Research* **2021**, 32, 144–150. https://doi.org/10.3103/S1068798X1202013X
39. Karpus, V.E.; Ivanov, V.A. Choice of the optimal configuration of modular reusable fixtures. *Russian Engineering Research* **2012**, 32, 213–219. https://doi.org/10.3103/S1068798X12030124
40. Kusyi, Y.; Onysko, O.; Kuk, A.; Solohub, B.; Kopei. V.; Development of the Technique for Designing Rational Routes of the Functional Surfaces Processing of Products. In: Karabegović I. (eds) *New Technologies, Development and Application V. NT 2022. Lecture Notes in Networks and Systems,* LNNS, Value 472. pp.135–143. https://doi.org/10.1007/978-3-031-05230-9_16
41. Kusyi, Y.; Stupnytskyy, V.; Onysko, O.; Dragašius, E. Optimization synthesis of technological parameters during manufacturing of the parts. *Eksploat. I Niezawodn.* **2022**, *24*, 655–667 https://doi.org/10.17531/ein.2022.4.6

 doi:10.20944/preprints202603.0123.v1

42. Jasiulewicz-Kaczmarek, M.; Antosz, K.; Zhang, C.; Ivanov, V. Industry 4.0 Technologies for Sustainable Asset Life Cycle Management. *Sustainability* **2023**, 15(7), 5833. https://doi.org/10.3390/su15075833
43. Onysko, O.; Panchuk,P.; Kopey, V.B.; Havryliv, Y.; Sculiar, I.; Investigation of the influence of the cutter-tool rake angle on the accuracy of the conical helix in the tapered thread machining. *International Conference on Applied Sciences. IOP Publishing Journal of Physics*: *Conference Series* **2021**, 1781,012028 https://doi.org/10.1088/1742-6596/1781/1/012028
44. Costa, C.E.; Polli, M.L. Effects of the infeed method on thread turning of AISI 304L stainless steel. *J. Braz. Soc. Mech. Sci. Eng*. 2021, *43*, 253. https://doi.org/10.1007/s40430-021-02978-7
45. Qing, Long, An; Guo, Giang, Guo; X.H. Zheng; Ming, Chen; Gang, Liu; Yun, Shan, Zhang. Experimental Study on Cutting Characteristics for Buttress Thread Turning of 13%Cr Stainless Steel. *Key Engineering Materials* **2010,** 443, 262-267 . https://doi.org/10.4028/www.scientific.net/KEM.443.262
46. Koleva, S.; Enchev, M.; Szecsi, T. Compensation of the deviations caused by mechanical deformations during machining of threads. *Procedia Manuf.* **2017**, *13*, 480–486. https://doi.org/10.1016/j.promfg.2017.09.066
47. Li, Z., Fu, X., Li, J. *et al.* Establishment of vibration wear model for turning large-pitch thread tools and its wear suppression method. *Int J Adv Manuf Technol* **2020**, **109**, 857–876. https://doi.org/10.1007/s00170-020-05403-w
48. Fu, X.; Li, K.; Li, Z. *et al.* A SVM-based design method for cutting edge profile stability of large-pitch thread turning tool considering vibration. *Int J Adv Manuf Technol* **2023**, 125, 4529–4547 https://doi.org/10.1007/s00170-023-10985-2
49. Khani, S.; Shahabi, Haghighi S.; Razfar, M. R.; Farahnakian, M. Improvement of thread turning process using micro-hole textured solid-lubricant embedded tools. *Proceedings of the Institution of Mechanical Engineers, Part B: Journal of Engineering Manufacture* **2021**, 235(11), 1727-1738. https://doi.org/10.1177/09544054211019929
50. Medvid, I.; Onysko, O.; Panchuk, V.; Pituley, L.; Schuliar, I. Kinematics of the Tapered Thread Machining by Lathe: Analytical Study. In *Lecture Notes in Mechanical Engineering*, Advanced Manufacturing Processes II. InterPartner 2020; Tonkonogyi, V., et al. Eds.; Springer: Cham, Switzerland, 2021; pp. 555–565. https://doi.org/10.1007/978-3-030-68014-5_54
51. Krawczyk, B; Szablewski, P; Mendak, M; Gapiński, B; Smak, K; Legutko, S; Wieczorowski, M; Miko, E. Surface Topography Description of Threads Made with Turning on Inconel 718 Shafts. *Materials* **2022,** 16(1), 80. https://doi.org/10.3390/ma16010080
52. Zawada-Tomkiewicz, A.; Żurawski, Ł.; Tomkiewicz, D.; Szafraniec, F. Sustainability and tool wear of titanium alloy thread cutting in dry and cryogenic conditions. *The International Journal of Advanced Manufacturing Technology* **2021**, 114, 2767–2781. https://doi.org/10.1007/s00170-021-07034-1
53. Slătineanu, L.; Radovanovic, M.; Coteață, M.; Beșliu, I.; Dodun, O.; Coman, I.; Olaru, S.-C. Requirements in designing a device for experimental investigation of threading accuracy. *MATEC Web of Conferences* **2017**. 112. 01005. https://doi.org/10.1051/matecconf/201711201005
54. Onysko, O.; Kopei, V.; Barz, C.; Kusyi, Y.; Baskutis, S.; Bembenek, M.; Dašić, P.; Panchuk, V. Analytical Model of Tapered Thread Made by Turning from Different Machinability Workpieces. *Machines* **2024**, 12, 313.https://doi.org/10.3390/machines12050313
55. Kopey V. B.; Onysko O. R.; Panchuk V. G. Computerized system based on FreeCAD for geometric simulation of the oil and gas equipment thread turning. *IOP Conf. Series: Materials Science and Engineering* **2019**, 477, 012032 https://doi.org/10.1088/1757-899X/477/1/012032
56. Balajti, Z.; Mándy, Z. Proposed solution to eliminate pitch fluctuation in case of conical screw surface machining by apex adjustment. *Procedia Manufacturing*, **2021**, https://doi.org/10.1016/j.promfg.2021.10.038
57. Onysko O.; Kopey V.; Panchuk V.; Medvid I.; Lukan T. Analitical Study of the kinematic rake angles of the cutting edge of the lathe tool for the tapered thread manufacturing «InterPartner» 2019. LNME, Odesa. P.236–245. https://doi.org/10.1007/978-3-030-40724-7_24
58. Máté, M.; Hollanda, D. About the Profile Accuracy of the Involute Gear Hob. *Acta Universitatis Sapientiae, Electrical and Mechanical Engineering*. **2017**, 9, 5–18. https://doi.org/10.1515/auseme-2017-0006

 doi:10.20944/preprints202603.0123.v1

59. Yao, X; Cui, J; Yu, H; Qi, X; Mi, X; Jiang, Y; Wang, M; Li, X. An improved accuracy-measuring method in manufacturing the lead screw of grating ruling engine, *Precision Engineering* **2017**, 49, 344-353. https://doi.org/10.1016/j.precisioneng.2017.03.004
60. V. Prokopiv, I. Horichok, T. Mazur, O. Matkivsky and L. Turovska, "Thermoelectric Materials Based on Samples of Microdispersed PbTe and CdTe," *2018 IEEE 8th International Conference Nanomaterials: Application & Properties (NAP)*, Zatoka, Ukraine, 2018, pp. 1-4, https://doi.org/10.1109/NAP.2018.8915357
61. Dzundza B., Kostyuk O., Mazur T. Software and Hardware Complex for Study of Photoelectric Properties of Semiconductor Structures. 2019 IEEE 39th International Conference on Electronics and Nanotechnology, ELNANO 2019 - Proceedings, art. no. 8783544, pp. 635 - 639, https://doi.org/10.1109/ELNANO.2019.8783544
62. Tolvaly-Roşca, F.; Máté, M.; Forgó, M; Z.; Pásztor, J. CAD solution to determine points from chipping tool solid model cutting edges. *Műszaki Tudományos Közlemények* **2020**, 12, 67–70. https://doi.org/10.33894/mtk-2020.12.10
63. Martins, F.S.; Reina-Muñoz, R.; Lira, V.M.; System of cutting force data acquisition in mechanical lathes *DYNA* **2018**, 85(207), 16 https://doi.org/10.15446/dyna.v85n207.67537
64. Demirpolat, H.; Binali, R.; Patange, A.D.; Pardeshi, S.S.; Gnanasekaran, S. Comparison of Tool Wear, Surface Roughness, Cutting Forces, Tool Tip Temperature, and Chip Shape during Sustainable Turning of Bearing Steel. *Materials* **2023**, 16, 4408. https://doi.org/10.3390/ma16124408
65. Lubis, S.; Rosehan; Darmawan, S.; Indra, B. *et* Tool Wear Analysis of Coated Carbide Tools on Cutting Force in Machining Process of AISI 4140 Steel. *IOP Conf. Ser.: Mater. Sci. Eng.* **2020**, 852, 012083. https://doi.org/10.1088/1757-899X/852/1/012083
66. Sandvik Coromant. Tread Turning Tools. URL: https://www.sandvik.coromant.com/en-us/tools/threading-tools/thread-turning-tools (accessed on 28 February 2026).
67. Sun, L., Cui, X., Wang, C., Zhang, Y., Li, C. Mechanical behavior of material removal under various rake angle diamond tool ultra-precision cutting of titanium alloy. Journal of Materials Research and Technology. 2025. 38. P.1302-1312. https://doi.org/10.1016/j.jmrt.2025.07.225
68. Rake Angle Versus Material. Thread Check Inc. URL: https://www.threadcheck.com/rake-angle-versus-material/
69. Specification for Threading and Gauging of Rotary Shouldered Thread Connections. ANSI/API SPECIFICATION 7-2 (formerly in SPEC 7). First edition, 2008. https://www.api.org/~/media/files/publications/addenda-and-errata/exploration-production/7_2_add_1.pdf?la=en
70. GOST 50864-96. Tool-joint tapered thread for drill string elements. Profile, dimensions, technical requirements.
71. GOST 9484–81. Basic norms of interchangeability. Trapezoidal screw thread. Profiles.
72. Acme Screw Threads. B1.5 - 1997 (R2024). ASME. 1997. 124 p.
73. ISO metric trapezoidal screw threads — Basic dimensions. International Standard ISO 2904:2020.
74. Buttress Inch Screw Threads. ASME B1.9-1973 (R2025).
75. Casing and Tubing. API Specification 5CT 11 edition. API. 2023.
76. Walter Tools. Thread Turning. https://www.walter-tools.com/en-us/products/turning/thread-turning
77. Workpiece Material Group. Dormer Pramet s.r.o. https://www.dormerpramet.com/cz/en/WMG
78. Ezugwu E.O., Okeke C.I., Machado A.R. High speed threading of inclusion-modified steels with coated carbide tools, *Journal of Materials Processing Technology*, Volume 86, Issues 1–3,1999, 216-225. https://doi.org/10.1016/S0924-0136(98)00313-6
79. A textbook of analytical geometry. H.D. Pandey, S.K.D. Dubey, M.Q. Khan, O.P. Dubey, Ajit Kumar is edition published by Dominant Publishers and Distributors (P) Ltd 4378/4-B Murarilal Street, Ansari Road, Daryaganj, New Delhi-110002. ISBN: 978-93-80642-14-7 https://wisdompress.co.in/wp-content/uploads/2022/10/A-Textbook-of-Analytical-Geometry.pdf
80. Privalov, I. I. Analytical Geometry. Moscow: Nauka, 2007. 394 p. (in Russian).

 doi:10.20944/preprints202603.0123.v1

81. Shervatov, V. G. Hyperbolic Functions. Moscow: State Publishing House of Technical and Theoretical Literature, 1953. 58 p. (in Russian) .
82. Kopei V., Onysko O. Threading_dev5.ipynb URL: https://colab.research.google.com/drive/1EVUOh9sPqzQxi8Loboyt_3rPYor7AedR